Rheology and Enhancement of Extrusion of Linear and Branched Polyethylenes Using Low Amount of Organoclay

Ayuba A. Adesina,[1] Abdulhadi A. Al-Juhani,[1] Nouar Tabet,[2] Anwar Ul-Hamid,[3] Ibnelwaleed A. Hussein[1]

[1]*Department of Chemical Engineering, King Fahd University of Petroleum and Minerals, 31261, Dhahran, Saudi Arabia*
[2]*Department of Physics, King Fahd University of Petroleum and Minerals, 31261, Dhahran, Saudi Arabia*
[3]*Research Institute, King Fahd University of Petroleum and Minerals, 31261, Dhahran, Saudi Arabia*

Received 2 June 2011; accepted 2 January 2012
DOI 10.1002/app.36722
Published online in Wiley Online Library (wileyonlinelibrary.com).

ABSTRACT: Interaction between 0.05 wt % organoclay and polyethylenes of different short chain branching (SCB) was studied. Linear rheology (van Gurp-Palmen plot) was used to study the effect of organoclay on the rheology of polyethylenes. Organoclay had effect only on the van Gurp-Palmen plot of linear polyethylene. Fourier transform (FT) rheology, extrusion at high-shear rates in a slit rheometer, transient stress growth analysis, and extensional rheology were conducted to examine the potential of organoclay as a processing aid. Organoclay reduced the transient stress overshoot, normal stress difference, ηo, onset of shear thinning, and extrusion pressure of polyethylene. The reduction was more pronounced in linear polyethylene without branching. Such effects gradually decreased as the branch content increased. The trend was independent of the type of flow (shear or extensional). It was interesting to note that FT rheology was not effective in explaining the impact of organoclay on polyethylene. The work concluded with the proposition that organoclay (as low as 0.05 wt %) was a good processing aid for linear polyethylene and polyethylenes with low content of SCB.
 J Appl Polym Sci 000: 000–000, 2012

Key words: organoclay; polyethylene; long chain branching; linear and nonlinear rheology

INTRODUCTION

Polymer–organoclay nanocomposites had attracted the attention of industrialists and researchers because of their different properties enhancement as compared with virgin polymers. The credit went to the inclusion of organoclay in the polymers. Enhanced mechanical and rheological properties, decreased gas permeability, increased heat resistance, and reduced permeability were some of the unique features of these nanocomposites.[1–6] These improvements were achieved at relatively low clay loading of 1–10 wt %.[7] Further, Hatzikiriakos et al.[8] and, recently, Adesina and Hussein[9] showed that addition of low loading (0.05–1 wt %) of organoclay could shift polyolefin melt instabilities, especially gross melt fracture, to higher shear rate. Also, Lee et al.[10] obtained novel blown-film polyethylene-clay nanocomposite foams with a clay loading of less than 1 wt % in the presence of supercritical carbon dioxide.

Rheology is often used as an analytical tool to study the behavior of polymer melt in processes such as extrusion[8] and injection molding.[11] Indeed, it is related to processability in many aspects and it plays a key role in optimizing polymer processing operations.[12,13] So, many publications investigated the effect of dispersion and clay loading on the melt flow properties of polyolefin-organoclay-based nanocomposites. Above percolation threshold,[13–16] organoclay was reported to have strong effects on linear and nonlinear rheology of the polymer matrix.[11] Generally, organoclay contributed to the increase in viscosity and elasticity of the host matrix.[11] For small angle oscillatory shear experiment, the storage modulus in the terminal regime was a solid-like plateau. There was a shear thinning at low-shear rate where the host polymer matrix would ordinarily have a zero-shear viscosity, ηo.[7,11,17] The critical strain, at which rheological response became nonlinear, was reported to be dependent on clay loading and extent of exfoliation and shifted to lower values with increasing solid volume fraction of organoclay.[17–19] The clay loading considered in all the

Correspondence to: I. A. Hussein (ihussein@kfupm.edu.sa).
Contract grant sponsor: King Abdul Aziz City for Science and Technology (KACST); contract grant number: AT-27-107.
Contract grant sponsor: King Fahd University of Petroleum and Minerals (KFUPM).

above mentioned cases was above 1 wt %. Treece et al.[16] showed that low clay loadings and poor exfoliation did not show shear thinning at low-shear rates but modest increase in the ηo due to the inclusion of the solid particles. Hatzikiriakos et al.[8] reported that the presence of organoclay causes a small decrease in the linear viscoelastic properties of the polymer for low concentration of 0.1 wt % and in many cases this difference may not be noticed. They concluded, based on the frequency sweep test, that organoclay had no effect on the shear rheology of the host polymer.[8] Furthermore, low clay loading (<0.5 wt %) reduced the extensional stresses in polymers at high Hencky strain rates.[8] Organoclay, at less than 0.5 wt %, was suggested as a good processing aid because of its ability to reduce the high-shear[9] and extensional stresses.[8,9] It is apparent that many issues are yet to be resolved regarding the impact of low organoclay loading on the rheology of polyolefins. For instance, the authors[9] showed that there is a reduction in steady shear viscosity at low-shear rates with the addition of organoclay. Can this effect be bulk-related or interfacial slip of the nanocomposite melt at the wall? This issue becomes more important when a shift in the flow curve of some polymers toward lower shear stress was observed during capillary extrusion.[8]

Moreover, it is generally accepted that extrusion of polyolefins involves several types of melt instabilities at high-shear rates. These instabilities are functions of many factors including the topology, molecular weight, polydispersity index (PDI), and branch content (BC) of the polymers among others. For instance, according to Filipe et al.,[20] materials with high-molecular weights and PDI were more prone to stick-slip instabilities while low-molecular weight and PDI polymers were often presented with sharkskin. Several authors had also shown that BC had significant influence on the structure and morphology of polyethylenes.[20–24] Palza[25] considered the interaction between comonomer content in polypropylene and clay in the presence of a compatibilizer. However, the clay loading in their work was 5 wt %. So, an increase in modulus of the polypropylene nanocomposite was reported. As far as we know, the effect of low clay loading on the melt rheology and extrusion of polyethylene was not carried out systematically. So, this article will try to consider the interaction between organoclay and the topology of polyethylene especially the short chain branching (SCB) and its distribution. Fourier transform (FT) rheology was successfully used to characterize different linear and branched commercial polyethylenes especially in the nonlinear flow regimes.[20,26–29] It was found to be sensitive to structural changes especially at the onset of nonlinearity.[30] So, in this work, we will employ FT rheological tools as well to analyze the effect of low clay loading on the different commercial polyethylenes in an effort to relate this to their extrusion in the presence of low amount of organoclay.

We used only, in this article, 0.05 wt % concentration because our main target was investigating the applicability of nanoclays as a processing aid additive for polyethylene. Most commercially used processing aid additives were used in industry in very low loading, usually expressed in ppm. Having a high loading of nanoclays would not be useful as a processing aid since it would increase the viscosity of polyethylene due to the hydrodynamic effect. Also, there were a lot of articles published on the rheology of polymer nanocomposites at high loading of nanoclay, where they usually reported the network formation of nanoclays at high loading by observing a plateau formation in G' versus frequency at small frequency range, and from this observation, they determined the rheological percolation threshold. However, this was not our objective, where we focused on the rheology of polyethylene nancomposites at very low loading of nanoclays, for the purpose of applying nanoclays here as a processing aid additive, where information on this aspect is scare in literature. The clay loading used in this study was 0.05 wt % because this ratio gave the most promising result as discussed in our recent publication.[9]

EXPERIMENTAL

Materials

HDPE and five linear low-density polyethylene (LLDPE) samples of different SCB, type of catalyst, and comonomer were used in this study. All samples were commercial resins produced by Exxon-Mobil. Two commercial metallocene ethylene–butene (EB) LLDPEs of different SCB (13 and 19 CH_3/1000 C) and two commercial ethylene–octene (EO) LLDPEs of different SCB (16 and 33 CH_3/1000 C) were tested to examine the influence of SCB and comonomer type. The LLDPEs were selected such that they have similar melt index (MI), density and weight-average molecular weight. On the other hand, one Ziegler–Natta (ZN) LLDPE was selected for a comparison with m-LLDPE to examine the influence of composition distribution. Here, the overall objective was to investigate the interaction of organoclay with polyethylene based on the composition distribution and BC while other molecular parameters were kept very similar. Table I provides characterization data for all the six samples. The properties such as weight-average molecular weight (M_w) and PDI were determined by gel permeation chromatography (GPC) and SCB was determined by

TABLE I
Investigated Polyethylene Samples: Density, Peak Melting Temperature (T_m), MI, Weight-Average Molecular Weight (M_w), PDI, and BC as the Total Number of Short Branches Determined by NMR

Polymer sample	Density (g/cm^3)	Peak melting temperature (°C)	MI (g/10 min)	M_w (kg/mol)	PDI	BC (CH_3/1000C)
HDPE_L	0.961	140	0.7	102	6.71	0
ZN-EB13	0.918	120	1	118	3.07	13.2
m-EB15	0.91	104	1.2	108	1.95	14.5
m-EB19	0.9	92	1.2	110	1.78	18.5
m-EO16	0.902	97	1.1	90	2.04	16.32
m-EO33	0.882	70	1.1	95	1.99	32.67

^{13}C-NMR. GPC data was collected using 1,2,4-trichlorobenzene as solvent at 150°C in a WATERS GPC2000 (USA) instrument equipped with refractive index, infra red, and viscosity detectors. Polystyrene standards were used for calibration. Details of GPC and NMR characterization were given elsewhere.[31] Density, peak melting temperatures, and MI data were provided by the manufacturer. The sample name reflected its catalyst type (metallocene or ZN), comonomer type (EB or EO) and contained a number that indicated its SCB (CH_3/1000 C). For example, m-EB19 was a metallocene ethylene–butene copolymer with a SCB of 19 CH_3/1000 C.

The organoclay used in this work was Cloisite(R) 15A (C15A) from Southern Clay, USA. The surfactant in the organoclay was di-methyl, dehydrogenated tallow, quaternary ammonium. It had a d_{001} spacing of 31.5 Å. A total of 0.05 wt % of C15A was used in the preparation of the polyethylene-organoclay nanocomposites. So, m-EB15-C15A means metallocene ethylene butene copolymer with SCB of 15 CH_3/1000 C containing 0.05 wt % C15A as organoclay processing additive.

Melt blending and morphology characterization

The Brabender 50 EHT mixer supplied with the Plastograph (Brabender® GmbH & Co., Germany) was used in the preparation of the nanocomposite. The organoclay was first heated in a vacuum oven at 108°C for more than 24 h to remove physico-adsorbed water. The grounded polymer sample was pre mixed with organoclay before introduced into the mixer using manual feeder. The blending was done for 10 min at 50 rpm. The blending temperature for each sample was 50°C above its peak melting temperature. Addition of 0.1 wt % of antioxidant (AO) to the nanocomposite during melt blending was necessary to prevent thermal degradation. The AO was a 50/50 blend of Irganox 1010 and Irgafos 168 from Ciba-Geigy Specialty, Switzerland. The pure samples were also processed in the Brabender 50 EHT mixer under similar conditions

The structure of the PE/organoclay nanocomposites was characterized by Nova™ NanoSEM 230 (FEI, USA). Nova™ NanoSEM 230 was a field emission scanning electron microscope. It was configured to get information down to nanometer level on non-conductive materials. The SEM samples were made from a thin film and etched for 4 h. The etching solution was made from a solution of H_2SO_4/H_3PO_4/H_2O (10/4/1) and 0.01 g/mL $KMnO_4$ as detailed in Ref. 9. The etched samples were sputter coated with gold for 90 s using Fine Coat Ion Sputter JFC–1100 (JEOL, Tokyo, Japan). Figure 1(a,b) shows SEM micrographs for HDPE-L and HDPE-L-C15A, respectively. The results showed that there was a fair distributive dispersion of organoclay in polyethylene with master batch-dilution technique. Similar results were shown in our previous publication.[9] The samples for tests in ARES rheometer (TA Instruments, USA) were prepared from melt-blended samples at a temperature of 50°C above the melting temperature (T_m) of the polymers. The pressure of up to 30 Pa was applied in a Carver press. The disc samples with dimensions of 25-mm diameter and 2-mm thickness were prepared for shear rheology.

Rheological measurements

ARES controlled strain rheometer (TA Instruments) was used for all rheological measurements. It was equipped with heavy transducer (range 0.02–20 N for normal force; 2×10^{-5} to 2×10^{-1} Nm for torque). The linear and nonlinear viscoelastic experiments were performed using 25-mm parallel plates. The plates were heated for at least 20 min to stabilize the temperature. For reproducibility of results, a presteady shear rate of 0.1 s^{-1} was applied for 20 s for all the tests in the parallel plates and time delay of 100 s before the actual tests. Different rheological tests were conducted to study the material properties under different rheological conditions. The tests were performed at a temperature of T_m + 50°C for different samples. The variation in the testing temperature was to prevent differences in the melt state properties of the samples as previously explained by Palza et al.[32] The differences could arise from dissimilarity in BC and molecular weight.

Strain sweep tests were done on each sample to determine the linear regime. Sample results on

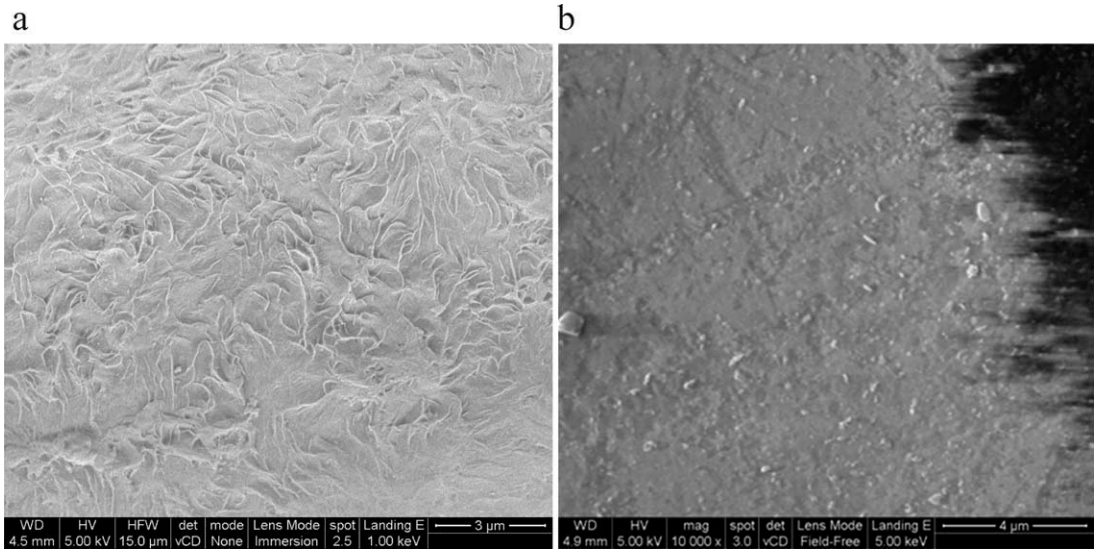

Figure 1 Scanning electron micrograph for (a) HDPE-L and (b) HDPE-L-C15A.

HDPE-L and ZN-EB13 and their nanocomposites were as presented in Figure 2. Generally, a strain of 10% within the linear regime was chosen for frequency sweep tests on all the samples. The frequency was varied from 0.1 to 100 rad/s. Most of the experiments were repeated three times. The maximum deviation was less than 5% from the mean. Then, van Gurp-Palmen plot [δ(arctan G''/G') versus complex modulus, G^*] was used to investigate the effect of organoclay on the rheology of polyethylene.

FT rheology was conducted at a frequency of 0.1 Hz for a strain range 10–400%. Raw torque data from ARES rheometer was digitized using 16-bit analog-to-digital converter card from National Instruments. In this work, sampling rate of 200 data points per cycle was used. Details of the experimental work can be seen elsewhere.[33] It had been shown

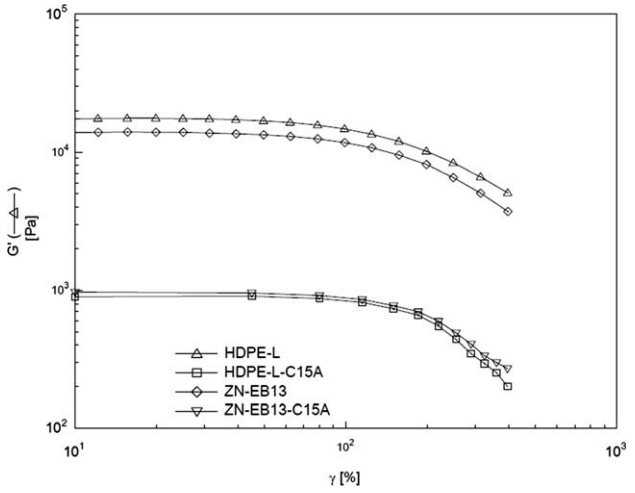

Figure 2 Elastic modulus versus strain for HDPE-L and ZN-EB13 and their nanocomposites.

that the shear stress response involves harmonics. The intensities and phases of such harmonics were used in the characterization of nonlinearity in the polymer. Most importantly the relative intensity of the second harmonic ($I_{2/1}$), relative intensity of the third harmonic ($I_{3/1}$) and relative phase angle of the third harmonic (Φ_3) were found very useful in such analysis.[33,34] They were defined as:

$$I_{3/1} = \frac{I(3w_1)}{I(w_1)} \tag{1}$$

$$I_{2/1} = \frac{I(2w_1)}{I(w_1)} \tag{2}$$

and

$$\Phi_3 = \varphi_3 - \varphi_1 \tag{3}$$

where $I(2w_1)$, $I(3w_1)$, and φ_3 are the shear stress intensity of the second and third harmonics and phase angle of the third harmonic, respectively. $I(w_1)$ and φ_3 are the shear stress intensity and phase angle of the first harmonic, respectively. Most of the experiments were repeated three times. The maximum deviation in $I_{3/1}$ and $I_{2/1}$ were found to be less than 5% of the mean and less than $\pm 5^\circ$ around the mean for Φ_3.

Another important shear test conducted was stress growth experiment. This was done to examine the effect of organoclay on the polyethylene during a transient shear process. A step shear rate of 1 s^{-1} was applied on the samples placed between the parallel plates (1 mm apart). The applied shear rate was kept constant for 200 s. The results were reproducible with maximum deviation of 10% around the mean.

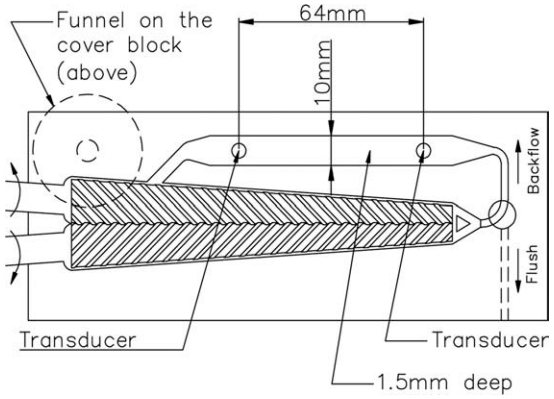

Figure 3 Longitudinal section of MiniLab™: A mini twin screw extruder with slit die along its backflow channel.

Furthermore, extrusion pressure at relatively high-shear rates was studied in a continuous MiniLab™ II Rheomex CTW5 (Thermo Scientific Germany) shown in Figure 3. The MiniLab™ consists of conical counter rotating twin screw with backflow channel. The backflow channel was designed as a slit capillary (64 mm × 10 mm × 1.5 mm) with two pressure transducers at the capillary entrance and exit. The maximum allowable pressure at the entrance and exit of the backflow channel are 200 and 100 bar, respectively. The maximum obtainable screw speed is 360 rpm. To study the effect of organoclay on the extrusion pressure, the speed of the screw was varied from 20 to 300 rpm at a temperature ~ 50°C above the melting point of each sample. The samples were introduced into the MiniLab™ in three steps with 2–3 mL fed-in during each step. It should be noted that the MiniLab™ was only good for comparative studies between samples. This was due to the inaccessibility to the actual extruded sample volume during the rheometry study. The developed melt flow instabilities during the rheometry were as well not observable due to the MiniLab™ mode of operation. Despite the instabilities, there did exist good reproducibility of results. As found in this work, the results were reproducible with maximum deviation of ±4% around the mean for all the allowable shear rates. Crossmodel [eq. (4)] served as a good regression model for the obtained flow curve.

$$\tau = \dot{\gamma}\frac{\eta_o}{1 + (\dot{\gamma}/\dot{\gamma}_b)^n} \tag{4}$$

τ (Pa) is the shear stress while $\dot{\gamma}$ (s^{-1}) is the apparent shear rate. η_o is in Pa s and n is the crossrate constant (dimensionless), and $\dot{\gamma}_b$ (s^{-1}) is the critical shear rate at the onset of shear thinning.

The extensional viscosity fixture (EVF) in ARES rheometer was used in the study of extensional rheology. The sample was pre stretched with a strain rate of 0.04 (s^{-1}) to remove sagging. Then, it was left in the fixture for 3 min to relax any accumulated stress before the start of the experiment. The used Hencky strain rate was 20 (s^{-1}). Also, the extensional experiments were performed at a temperature

TABLE II
Investigated Samples: Testing Temperature, Crossover Modulus (G_c), and Longest Relaxation Time λ_c

Sample	Testing temperature (°C)[a]	G_c (MPa)	λ_c (s)[b]
HDPE-L	190	5.62×10^{-2}	0.107
HDPE-L-C15A	190	6.37×10^{-2}	0.083
ZN-EB13	170	1.64×10^{-1}	0.083
ZN-EB13-C15A	170	1.61×10^{-1}	0.081
m-EB15	160	2.46×10^{-1}	0.059
m-EB15-C15A	160	2.5×10^{-1}	0.059
m-EB19	150	2.33×10^{-1}	0.08
m-EB19-C15A	150	2.29×10^{-1}	0.08
m-EO16	150	1.34×10^{-1}	0.078
m-EO16-C15A	150	1.35×10^{-1}	0.077
m-EO33	120	1.13×10^{-1}	0.22
m-EO33-C15A	120	1.11×10^{-1}	0.216

[a] Testing temperature for each sample was approximately $T_m + 50$°C.
[b] The longest relaxation time determined when the elastic modulus is equal to loss modulus.

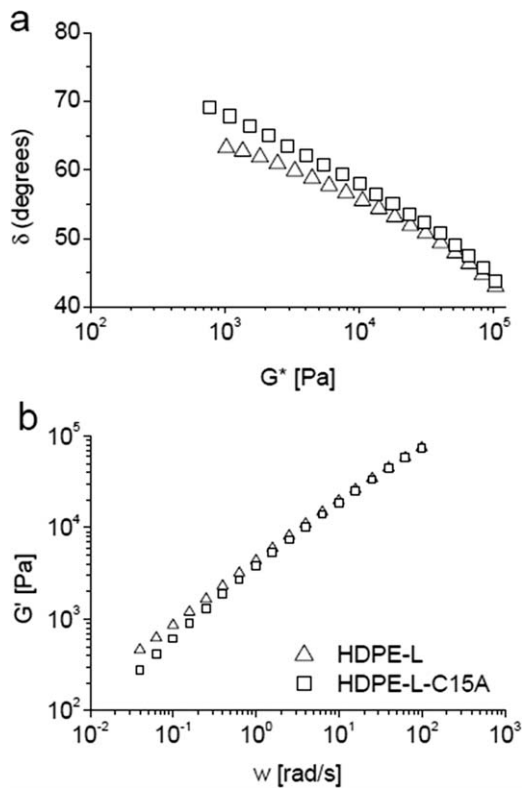

Figure 4 (a) van Gurp-Palmen plot and (b) elastic modulus versus frequency for HDPE-L and HDPE-L-C15A. The testing temperature was $T_m + 50$°C (190°C).

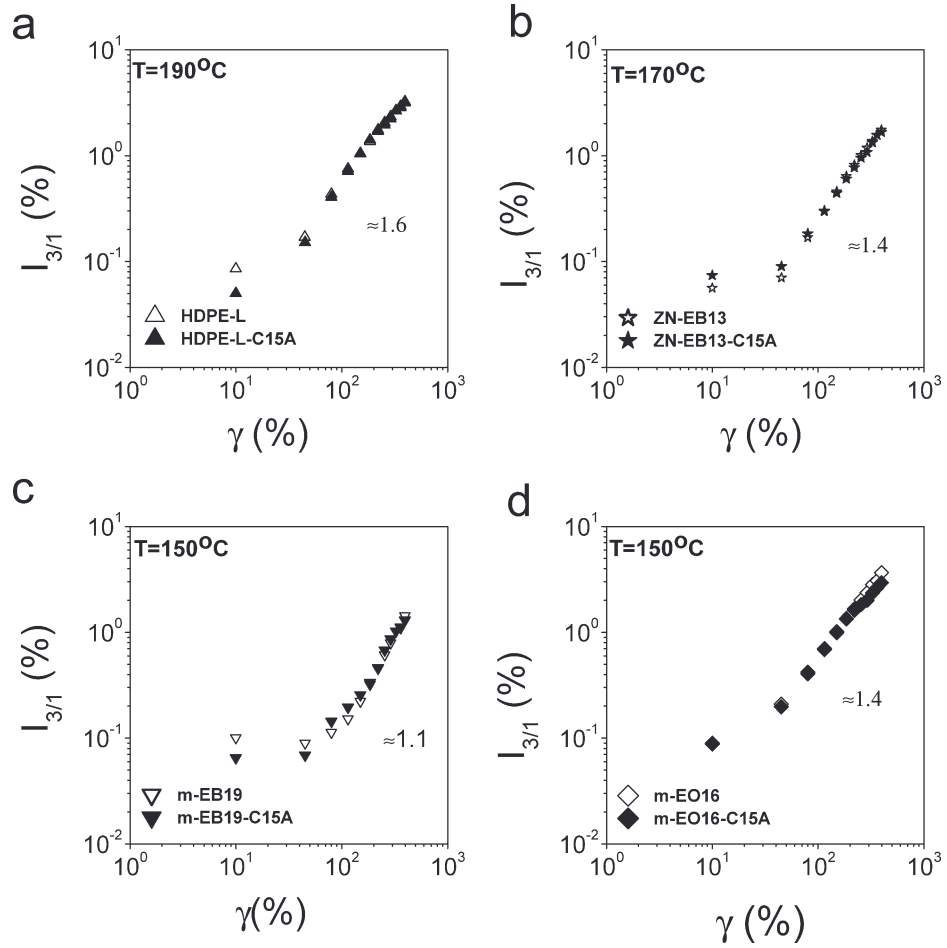

Figure 5 Relative intensity of the third harmonic as a function of strain amplitude at approximately $T_m + 50$°C for (a) HDPE-L and HDPE-L-C15A, (b) ZN-EB13 and ZN-EB13-C15A, (c) m-EB19 and m-EB19-C15A, and (d) m-EO16 and m-EO16-C15A.

of 15°C above the melting temperatures of the samples. The results were reproducible with maximum deviation of 10% around the mean.

RESULTS

Linear polyethylene (HDPE-L)

The results of dynamic shear tests were analyzed using TA Orchestrator (ARES software from TA Instruments) to obtain crossover modulus, G_c, and longest relaxation time (λ_c). The results are shown in Table II. G_c of HDPE-L increased by 13% while its λ_c decreased by 22% with the addition of organoclay. However, plateau modulus was not attained at the temperature used in this work. Figure 4(a) shows the van Gurp-Palmen plot of HDPE-L and HDPE-L-C15A. The shape of linear HDPE (HDPE-L) showed in the figure was similar to the linear polyethylene presented in the work of Vittorias and Wilhelm.[26] However, the curve was less steep as compared with the one reported by them.[26] The variation in the steepness was likely due to differences in the PDI of the linear polymers and testing temperatures in both works. Organoclay influenced the van Gurp-Palmen plot of HDPE-L. The effect was more pronounced below the crossover frequency. The plot of HDPE-L shifted upward. This was an indication that organoclay reduced the elasticity of the HDPE-L and hence the melt was more viscous as shown in Figure 4(b). The increase in G_c, the decrease in λ_c and the upward shift in van Gurp-Palmen plot of HDPE-L showed that organoclay had effect on the linear viscoelastic properties of linear polyethylene.

The effect of organoclay on $I_{3/1}$of all the polyethylenes was shown in Figure 5. Generally, the slope of the log–log plot of $I_{3/1}$ versus γ is less than 2. Figure 5(a) shows that relative amplitude of the third harmonic for both HDPE-L and HDPE-L-C15A was the same. Similarly, organoclay had no effect on the relative phase angle of the third harmonic (figure not shown) up to strain amplitude of 155%. Stress decay occurred above strain amplitude 155%. Such decay was an attribute of slip during large amplitude oscillatory shear.[20,35,36] $I_{2/1}$ has been reported to be sensitive to flow behaviors like wall slip.[37]

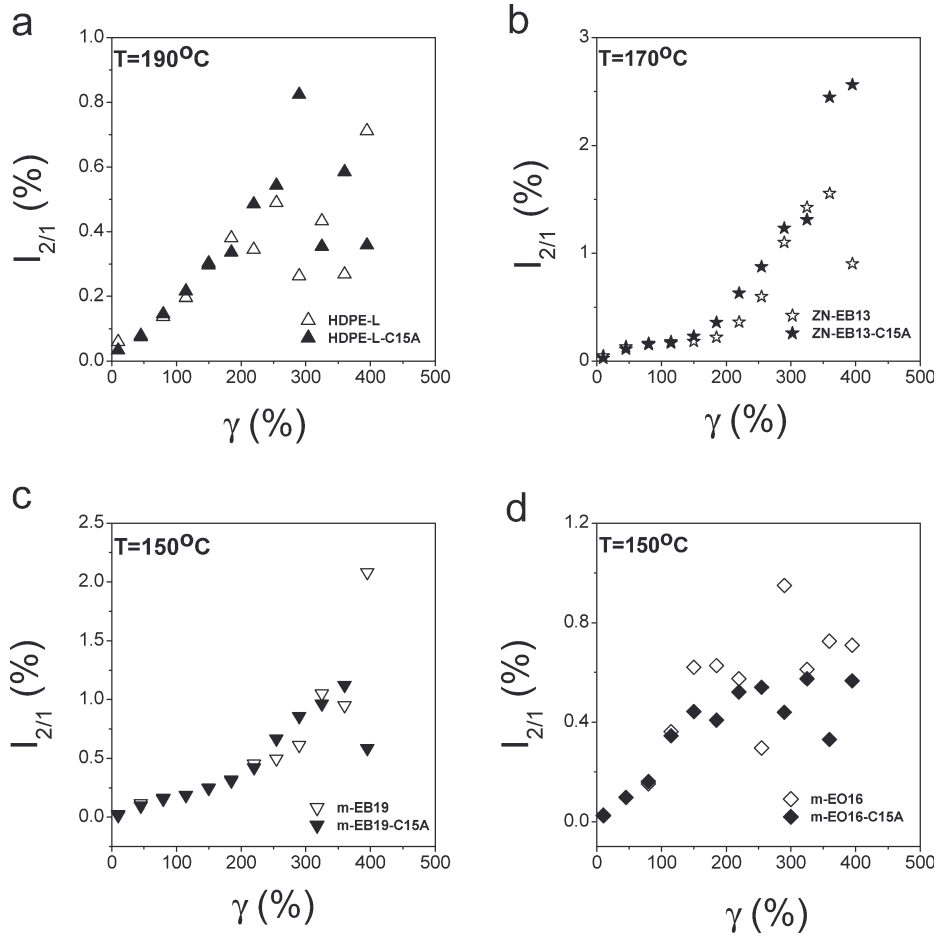

Figure 6 Relative intensity of the second harmonic as a function of strain amplitude at approximately $T_m + 50$°C for (a) HDPE-L and HDPE-L-C15A, (b) ZN-EB13 and ZN-EB13-C15A, (c) m-EB19 and m-EB19-C15A, and (d) m-EO16 and m-EO16-C15A.

Figure 6(a) shows that organoclay had no effect on $I_{2/1}$ of HDPE-L up to strain amplitude of 155%. Above this amplitude, there was a difference in the trend between HDPE-L and HDPE-L-C15A. However, no comment could be made on the trends because edge melt fracture was observed at the end of the experiment in all the cases.

Another important consideration during processing is the flow behavior of polymers during transient condition. One way to correlate rheology to processing is to perform transient stress growth experiment. The stress growth results for HDPE-L and HDPE-L-C15A were displayed in Figure 7. The overshoots in the stress growth and normal stress difference reduced with the inclusion of organoclay. At about 3.4 s after the start up of the stress growth test, the overshoot in stress growth reduced by 15% while the overshoot in normal stress difference of HDPE-L, at about 47.9 s, reduced by 28%. Such reduction in normal stress difference was an indication that organoclay reduced the elasticity of the melt which plays a major role in melt fracture of linear polyethylene. This subject was discussed in details in our previous work.[9]

Flow curves from MiniLab™ for HDPE-L and HDPE-L-C15A were shown in Figure 8. Addition of

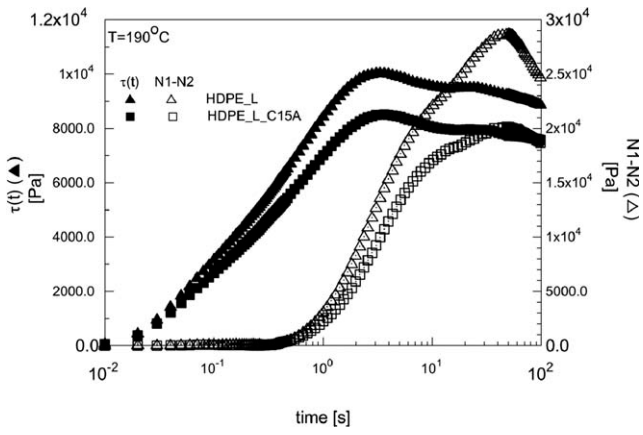

Figure 7 Transient shear stress and normal stress difference during stress growth test for HDPE-L and HDPE-L-C15A at 190°C.

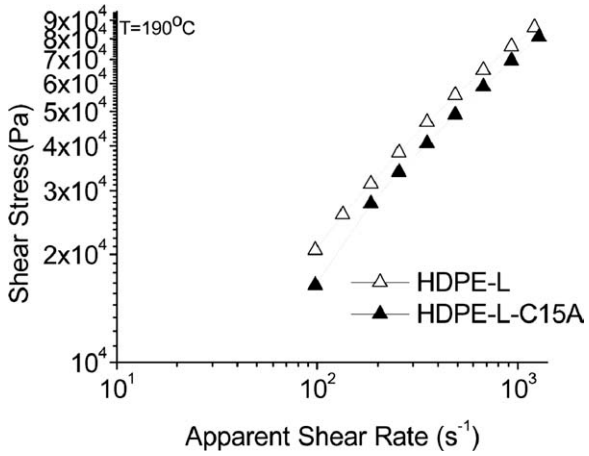

Figure 8 Flow curve for HDPE-L and HDPE-L-C15A at a temperature $T_m + 50°C$ (190°C).

0.05 wt % of organoclay to HDPE-L resulted in a decrease in the shear stress throughout the allowable range in MiniLab™. This implied a decrease in the extrusion pressure (more throughputs). Crossmodel in the form given in eq. (4) was used to quantify the extent of effect of organoclay on the flow curve of polyethylene at low clay loading. The results of the regression analysis were given in Table III. The reduction in η_o of HDPE-L was 23% in the presence of 0.05 wt % organoclay. However, the onset of shear thinning cannot be compared since the samples have different η_o. To resolve this problem, the degree of freedom in the crossmodel equation was reduced to two-based parameters by fixing the η_o as a constant. The results were displayed in Table III. The onset of shear thinning occurred at lower shear rate with the addition of 0.05 wt % of organoclay to HDPE-L. This was an indication that addition of low loading of organoclay to HDPE-L enhanced its processability.

It was previously confirmed that extensional behavior of polymer during melt extrusion is very important toward understanding the occurrence of melt instabilities.[8,38] Extensional flow plays an important role at the die exit. Reduction in extensional stress and strain at break may lead to the postponement of melt instabilities. The interaction of organoclay with HDPE-L was sensitive to extensional rheology as shown in Figure 9. The results showed that after 2.19 s, the addition of 0.05 wt % of organoclay reduced the maximum extensional stress in HDPE-L by 37%. The Hencky strain at break decreased from 3.9 to 3.49 with the addition of organoclay. So, for linear HDPE, we observed a decrease in both the extensional and normal stresses as a result of the addition of 0.05 wt % of organoclay. Further, organoclay caused a decrease in the extrusion pressure of HDPE-L.

ZN-based polyethylene (ZN-EB13)

Table II shows that the addition of 0.05 wt % organoclay had no effect on the crossover frequency and longest relaxation time of ZN-EB13. In general, 0.05 wt % organoclay had no effect on the linear viscoelastic properties of ZN-EB13. The relative amplitude [Fig. 5(b)] and phase angle (figure not shown) of the third harmonics of ZN-EB13 remained unchanged with the addition of organoclay. Up to the strain amplitude of 155%, the relative amplitude of the second harmonic was the same for ZN-EB13 and ZN-EB13-C15A [Fig. 6(b)]. As observed in the case HDPE-L, the differences in $I_{2/1}$ above 155% could not be discussed due to onset of edge melt fracture.

The effect of organoclay on transient stress growth of ZN-EB13 was shown in Figure 10. At about 3 s after the start up of the stress growth experiment, the overshoot in stress growth of ZN-EB13 reduced by 3% (not significant) while the overshoot in its normal stress difference at ≈9.4 s, reduced by 11%. It should be noted that the decrease in the normal

TABLE III
Crossmodel Parameters for all the Tested Samples

	Three-based Parameters			Two-based Parameters		
Sample	η_o (Pa s)	$\dot{\gamma}_b$ (s^{-1})	n	η_o (Pa s)	$\dot{\gamma}_b$ (s^{-1})	n
HDPE-L	345.4	178.4	0.71	345.4	178.4	0.71
HDPE-L-C15A	265.7	243.2	0.704	345.4	115.6	0.621
ZN-EB13	454.1	458.8	0.899	454.1	458.8	0.899
ZN-EB13-C15A	399.8	550.4	0.999	454.1	411.2	0.887
m-EB15	592.2	527.1	1.009	592.2	527.1	1.009
m-EB15-C15A	549.4	552	1.097	592.2	480.9	0.951
m-EB19	766.3	413.8	1.063	766.3	300	1.063
m-EB19-C15A	630.6	403	0.906	766.3	243.7	0.72
m-EO16	788.4	162.9	0.758	788.4	162.9	0.758
m-EO16-C15A	615.7	216.3	0.805	788.4	116.5	0.716
m-EO33	1415	87.54	0.765	1415	87.54	0.765
m-EO33-C15A	1392	94.03	0.787	1415	90.44	0.781

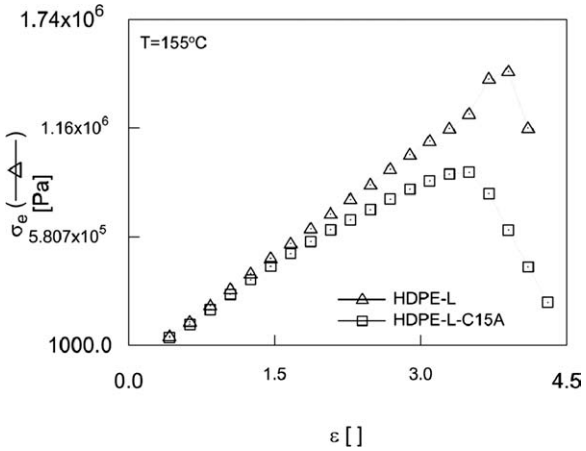

Figure 9 Extensional stress growth against extensional strain at Hencky strain rate of 20 s^{-1} and temperature of 155°C for HDPE-L and HDPE-L-C15A.

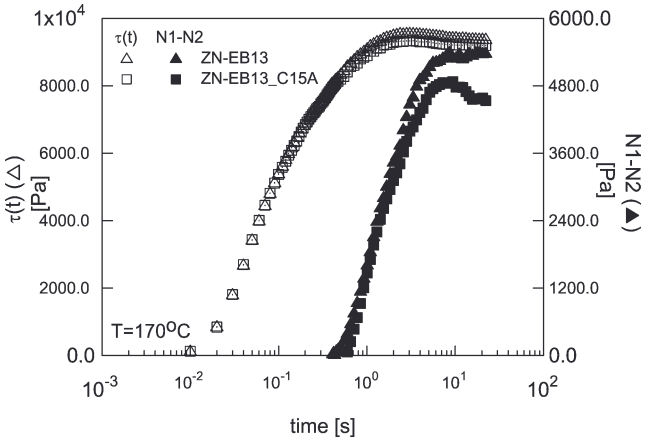

Figure 10 Transient shear stress and normal stress difference during stress growth test for ZN-EB13 and ZN-EB13-C15A at 170°C.

stress difference in ZN-EB13 due to organoclay inclusion was less than the decrease in HDPE-L. Organoclay's addition to ZN-EB13 resulted in the decrease in η_o of the polymer by 12%. The onset of shear thinning for ZN-EB13-C15A occurred at lower shear rate compared with ZN-EB13 (Table III). These results were similar to what occurred between HDPE-L and HDPE-L-C15A. Furthermore, the extensional stress in ZN-EB13 reduced by 16% while the Hencky strain at break decreased from 4.7 to 3.9 in the presence of 0.05 wt % organoclay (figure not shown). Similar trend was observed in the interaction between HDPE-L and organoclay. However, the influence of organoclay on HDPE-L was higher as compared with its impact on ZN-EB13.

Metallocene-based LLDPE

The results given in Table II suggested that the organoclay had no effect on the crossover modulus and longest relaxation time of metallocene-based polyethylenes. It also had no influence on their van Gurp-Palmen plots (figures not shown). Hence, organoclay's effect on the linear viscoelastic properties of metallocene-based polyethylene was negligible.

The influence of organoclay on the $I_{3/1}$ of metallocene-based polyethylenes was insignificant [Fig. 4(c,d)]. Below strain amplitude 155%, the slip behavior of metallocene-based polyethylenes and their corresponding organoclay nanocomposites was similar [Fig. 5(c,d)]. The trends above strain amplitude 155%, as observed in the cases of HDPE-L and ZN-EB13, could not be relied upon.

Similarly, the reduction in the stress growth and normal stress difference of metallocene-based polyethylene due to the inclusion of organoclay were insignificant. For example, Figure 11 shows the transient stress growth and normal stress difference of m-EO33 and m-EO33-C15A. At about 3 s after the start up of the stress growth test, the overshoot in stress growth in m-EO33 reduced by 7% while the overshoot in its normal stress difference at about 31.2 s, reduced by 9%. Because of data reproducibility as mentioned under experimental set-up, such reductions were negligible.

The MiniLab^{TM} experiments suggested that addition of organoclay to metallocene-based polyethylenes influenced η_o and the onset of shear thinning up to a certain content of SCB. For example, organoclay reduced the η_o of m-EB19 by 18% while the shear rate at which the onset of shear thinning occurred was reduced by 19% (Table III). However, the reduction of η_o in m-EO33 was $\sim$ 2%, while the shear rate at which shear thinning set-in remained unaffected by the addition of organoclay.

Figure 12 shows the extensional results of m-EO33 and m-EO33-C15A. Similar results were obtained for all metallocene-based polyethylenes. The

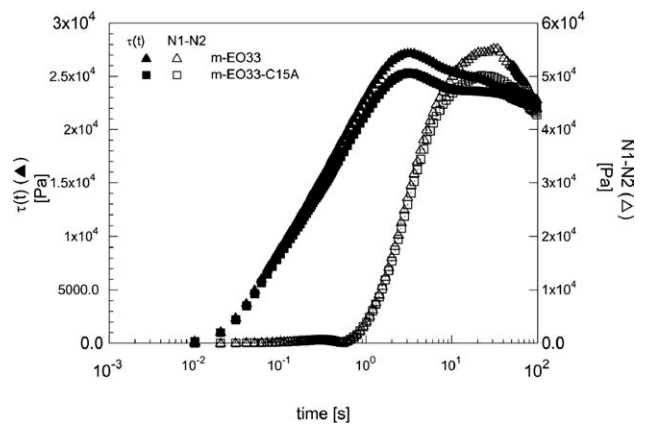

Figure 11 Transient shear stress and normal stress difference during stress growth test for m-EO33 and m-EO33-C15A at 120°C.

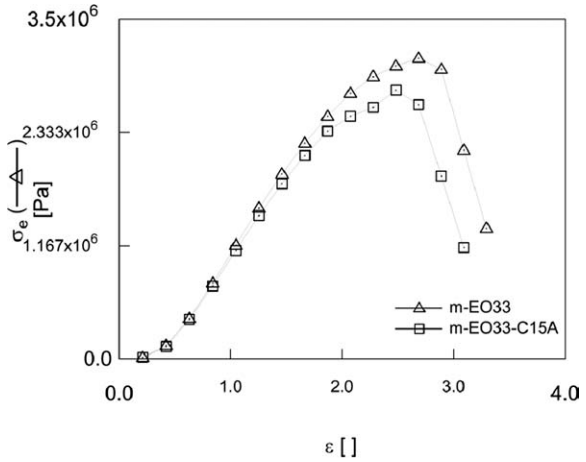

Figure 12 Extensional stress growth against extensional strain at Hencky strain rate of 20 s^{-1} and temperature of 85°C for m-EO33 and m-EO33-C15A.

reduction in extensional stress for metallocene-based polyethylenes in the presence of 0.05 wt % organoclay was less than 10%. The trend was independent of the type of comonomer. Such decrease was unreliable because of the issue of data reproducibility. The Hencky strain rate used in the experiment was 20 s^{-1}. Efforts to attain higher Hencky rate were futile because of the equipment limitation. It could be possible that the effect of organoclay on the metallocene-based polyethylene to be more noticeable at higher Hencky strain rates.

Further discussion

The results presented so far indicated that there was an interaction between organoclay and topology of polyethylenes especially the content of SCB. The impact of organoclay on HDPE-L was very obvious. Organoclay influenced both linear and nonlinear viscoelastic properties of linear polyethylene. Our tentative explanation for these observations was that the organoclay could easily streamline the flow and align in the flow direction. Similar observation was reported with respect to the inclusion of wood flour in HDPE. However, the wood flour, according to the authors, further migrated to the wall surface to initiate slip.[39–41] As the SCB increased, such streamlining and alignment in the flow direction became difficult. The effect was the same regardless of the type of catalyst, comonomer, and composition distribution. The trend in the interaction between organoclay and SCB was the same in both shear and extensional flows.

CONCLUSION

The effect of organoclay on the rheology and processing of polyethylenes of different SCB was studied. The results showed that organoclay did influence the linear viscoelastic properties of linear polyethylene. FT rheology was known to be very good for "finger printing" branching in polyethylenes,[20,26,33,42,43] its usefulness in studying the influence of organoclay on polyethylenes at low clay loading was, however, not successful. Organoclay did not induce more slip in the polyolefins as characterized by $I_{2/1}$. However, there is a need for further studies in this area to examine if organoclay could induce slip at high-shear flow. This becomes more necessary since at high-shear rates during extrusion, extrusion pressure of HDPE-L reduced in the presence of organoclay. Such reduction might be due to slip. This will be the focus of our future research. The transient stress overshoot and normal stress difference were reduced when 0.05 wt % organoclay was added to the linear polyethylene. Also, extensional stresses became dissipated in the presence of organoclay. The work concluded with the assertion that such effect became reduced as the SCB increased. In addition, the trend was independent of the type of flow. The results indicated that organoclay was likely to be a good processing aid in polyethylenes especially the linear polyethylene and polyethylenes with small SCB.

References

1. Emmanuel, P. G. Adv Mat 1996, 8, 29.
2. Krishnamoorti, R.; Vaia, R. A.; Giannelis, E. P. Chem Mater 1996, 8, 1728.
3. Wang, K. H.; Chung, I. J.; Jang, M. C.; Keum, J. K.; Song, H. H. Macromolecules 2002, 35, 5529.
4. Wang, K. H.; Xu, M.; Choi, Y. S.; Chung, I. J. Polym Bull 2001, 46, 499.
5. Susteric, Z.; Kos, T. Appl Rheol 2008, 18, 54894.
6. Katsikis, N.; Koniger, T.; Munstedt, H. Appl Rheol 2007, 17, 52751.
7. Solomon, M. J.; Almusallam, A. S.; Seefeldt, K. F.; Somwangthanaroj, A.; Varadan, P. Macromolecules 2001, 34, 1864.
8. Hatzikiriakos, S. G.; Rathod, N.; Muliawan, E. B. Polym Eng Sci 2005, 45, 1098.
9. Adesina, A. A; Hussein, I. A. J Appl Polym Sci 2012, 123, 866.
10. Lee, Y. H.; Wang, K. H.; Park, C. B.; Sain, M. J Appl Polym Sci 2007, 103, 2129.
11. Krishnamoorti, R.; Ren, J.; Silva, A. S. J Chem Phys 2001, 114, 4968.
12. Rosenbaum, E. E.; Randa, S. K.; Hatzikiriakos, S. G.; Stewart, C. W.; Henry, D. L.; Buckmaster, M. Polym Eng Sci 2000, 40, 179.
13. Wissbrun, K. F.; Dealy, J. M. Melt Rheology and Its Role in Plastics Processing: Theory and Applications; Springer: New York, 1999.
14. Gu, S. Y.; Ren, J.; Wang, Q. F. J Appl Polym Sci 2004, 91, 2427.
15. Jin, Z.; Alexander, B. M.; Joseph, D. H. Polymer 2005, 46, 8641.
16. Treece, M. A.; Oberhauser, J. P. J Appl Polym Sci 2007, 103, 884.
17. Ren, J.; Krishnamoorti, R. Macromolecules 2003, 36, 4443.
18. Jian, L.; Cixing, Z.; Gang, W.; Zhao, D. J Appl Polym Sci 2003, 89, 3609.
19. Thierry, A.; Tolotrahasina, R.; Médéric, P. J Rheol 2005, 49, 425.
20. Filipe, S.; Vittorias, I.; Wilhelm, M. Macromol Mater Eng 2008, 293, 57.

21. Hussein, I. A. Polym Int 2005, 54, 1330.
22. Hussein, I. A.; Hameed, T.; Sharkh, B. F. A.; Mezghani, K. Polymer 2003, 44, 4665.
23. Usami, T.; Gotoh, Y.; Takayama, S. Macromolecules 1986, 19, 2722.
24. Lohse, D. J.; Milner, S. T.; Fetters, L. J; Xenidou, M.; Hadjichristidis, N.; Mendelson, R. A.; Garc Ã-a-Franco, C. A.; Lyon, M. K. Macromolecules 2002, 35, 3066.
25. Palza, H. Macromol Mater Eng 2010, 295, 492.
26. Vittorias, I.; Wilhelm, M. Macromol Mater Eng 2007, 292, 935.
27. Filipe, S.; Becker, A.; Barroso, V.; Wilhelm, M. Appl Rheol 2009, 19, 23345.
28. Klein, C.; Venema, P.; Sagis, L. D. D.; Wilhelm, M.; Spiess, H. L. E.; Rogers, S.; Donald, A. Appl Rheol 2007, 17, 45210.
29. Wilhelm, M. Macromol Mater Eng 2002, 287, 83.
30. Wilhelm, M.; Reinheimer, P.; Ortseifer, M.; Neidhöfer, T.; Spiess, H. W. Rheol Acta 2000, 39, 241.
31. Hameed, T.; Hussein, I. A. Polymer 2002, 43, 6911.
32. Palza, H.; Filipe, S.; Naue, I. F. C.; Wilhelm, M. Polymer 2010, 51, 522.
33. Vittorias, I.; Parkinson, M.; Klimke, K.; Debbaut, B.; Wilhelm, M. Rheol Acta 2007, 46, 321.
34. Neidhofer, T.; Wilhelm, M.; Debbaut, B. J Rheol 2003, 47, 1351.
35. Chen, Y. L.; Larson, R. G.; Patel, S. S. Rheol Acta 1994, 33, 243.
36. Hatzikiriakos, S. G.; Dealy, J. M. J Rheol 1992, 36, 845.
37. Michael, D. G. J Rheol 1995, 39, 697.
38. Hatzikiriakos, S. G.; Migler, K. B. Polymer Processing Instabilities Control and Understanding; Marcel Dekker: New York, 2005.
39. Hristov, V.; Takács, E.; Vlachopoulos, J. Polym Eng Sci 2006, 46, 1204.
40. Becraft, M. L.; Metzner, A. B. J Rheol 1992, 36, 143.
41. Knutsson, B. A.; White, J. L.; Abbas, K. B. J Appl Polym Sci 1981, 26, 2347.
42. Schlatter, G.; Fleury, G.; Muller, R. Macromolecules 2005, 38, 6492.
43. Vega, J. F.; Santamar, Ã. A.; Muaoz, E. A.; Lafuente, P. Macromolecules 1998, 31, 3639.